International Journal of Research
Available at https://edupediapublications.org/journals
p-ISSN: 2348-6848
e-ISSN: 2348-795X
Volume 04 Issue 01
January2017

# EMI Reduction in DC-Fed Electric Drives by Active Common-Mode Compensator

Ms. Nimmakayala Kavitha ,kavithareddy233@gmail.com
A. Bhaktha Vachala[Ph.D], bhaktha1000@gmail.com

***Abstract*—A novel common-mode (CM) EMI active filter for dc-fed motor drives is proposed. The active filter performs both the compensation of the CM voltage at the motor input and the mitigation of the leakage high-frequency CM currents, thus increasing the drive reliability and the vehicle electromagnetic compatibility (EMC). The filter scheme is based on a voltage feedback action and also includes a feed-forward action by exploiting a suitably estimated CM current. An optimized design of the CM voltage detection/injection systems is implemented. Moreover, the active filter is supplied by a smaller voltage than the dc link value; this permits a more performing amplifier to be used. The active filter behavior is analyzed theoretically and its performance is assessed by experiments. The realized prototype shows a good efficiency and compactness.**

***Index Terms*—Active filter, electromagnetic conductive interference, induction motor drive, vehicles.**

## I. Introduction

DC-fed motor drives are currently used in a broad variety of applications. In particular, they are suited to vehicle applications (road and marine vehicles, aircrafts, etc.) and can be simply operated in a dc distribution system, such as in the case of some residential/commercial building dc grids [1], [2].

With reference to vehicles, the evolution of their electrical architectures has shown a growing use of electrical loads, such as drives and actuators. For example, the more electric vehicle (MEV) [3], [4] concept encourages the employment of electrical power systems aimed at a better use of the high power loads. This is possible due to the introduction of power electronics to optimize fuel economy, environmental emissions, performance, and reliability of the vehicles, including sea, undersea, and air vehicles [1]–[5]. Therefore, a massive use of switching power converters is expected to improve the flexibility of the load management and overall vehicle energy saving. On the other hand, as far as the pulsewidth-modulated (PWM) drives are concerned, two main problems are encountered, which are related to the inverter high switching frequency operation. The first is the electromagnetic interference (EMI) toward the on-board power supply lines that can degrade the operation of other sensitive devices and systems coexisting in the vehicle environment. The second problem is related to the drive reliability. Indeed, the CM voltage on the stator windings creates a shaft voltage by capacitive coupling through the motor air-gap, and consequently, electrostatic discharges are generated through the bearing lubricating film. The motor bearings suffer for such currents that are the cause of a dramatic reduction of the motor lifetime [6]–[8]. An additional problem is given by vibrations and noise generated by motor drives in both civil (passengers' comfort) and military (acoustic discretion) applications, producing bearing damage, which, in turn, amplifies the phenomenon.

The modern trend in the field of vehicle electrical architectures is towards the increase of electrical loads, such as drives and actuators. The X-by-Wire (XBW) technology, as well as the More Electric Vehicle (MEV) concept , are expressions of this trend. In particular, XBW technology is intended as the introduction of electronic systems into the vehicle to enhance and replace tasks previously accomplishedvia mechanical and hydraulic systems.

In addition, the MoreElectric Vehicle (MEV) emphasizes the employment ofelectrical power systems with the aim of a more rationale useof the high power loads thanks to the introduction of powerelectronics to optimize fuel economy, environmentalemissions, performance and reliability of the vehicles [1]-[3].

Technical literature exhibits several studies dedicated to the control and mitigation of the EMI in motor drives used both in industrial and in vehicular applications [9]–[28]. A comprehensive study, giving a generalization of harmonic and EMI active filters behavior, is presented in [9]. As for the reduction of EMI disturbance toward the supply line, a survey of EMI mitigation techniques is proposed in [10] and a comparative study of CM and differential mode (DM) active EMI filters compensation performance is proposed in [11]. As for the automotive environment, [12]–[14] suggest remedies based on the use of passive filters. In [15], [16] design criteria are proposed to optimize the performance and size of EMI passive filters, while in [17], an active hybrid filter is devised in which a CM active filter is used to reduce the size of the CM inductor of a passive EMI filter. In [18], a feed-forward, current-controlled, current-source active filter for CM noise cancellation is proposed, and in [19] and [20], a feedback current detecting and current compensating configuration of active filter is presented. As for the electromagnetic disturbance toward the motor, it should be noted that the reduction of CM EMI, in addition to the increase of the motor reliability, contributes also to the improvement of the electromagnetic compatibility (EMC), due to the reduction of common-mode ground current and of common-mode EMI emission toward the supply. In [21]–[24], feed-forward active CM filters are proposed to reduce CM voltage at the motor terminals. In [25], the effects of a feed-forward active compensation device for the attenuation of the CM voltage toward the motor in an induction vehicular motor drive are presented. Finally, a prototype of a feedback CM EMI filter for low voltage automotive drives has been developed in [26]. In [27], a further improvement of the filter described in [26] is proposed, being based on the introduction of an additional feed-forward action, based on a suitably estimated CM motor current. This paper extends and deepens

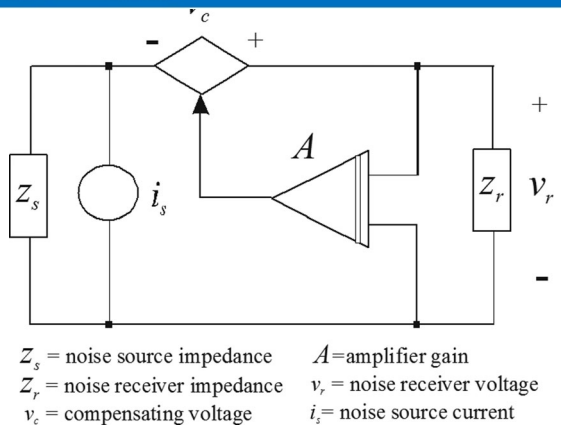


Fig. 1. Scheme of a feedback voltage-sensing voltage-compensating active filter.

the work developed in [27], presenting a theoretical analysis of the filter behavior, according to which the advantage of the additional feed-forward action, in terms of EMI suppression, is demonstrated. A more detailed description of the filter design, including the CM current estimator, is also given together with additional experimental results for the numerical evaluation of the improvement due to the feed-forward action. The considered application is a 1.1 kW, 42 V PWM vehicular induction motor drive, even if it can be applied to other voltage levels by a suitable choice of the power amplifier. The filter scheme is of the voltage-sensing voltage-compensating type with a new design of the CM voltage detection and injection systems. The feed-forward action is introduced enhancing the performance of the proposed circuit both in terms of motor CM voltage reduction and in terms of EMI mitigation in the frequency range between 10 kHz and 1 MHz. Furthermore, according to a design oriented to the optimization of the power to size ratio, a compact layout is obtained.

## II. Design Criteria of the Active Filter

### A. Choice of the Active Filter Scheme

Classifications of the active filter topologies, used in controlling EMI, are given in [9], [11], and [30]. According to these classifications, the proposed circuit is a feedback voltage-sensing, voltage-compensating type, shown in Fig. 1, and it behaves as a Butterworth low-pass filter. The main advantage of this choice lies on the good performance of the considered scheme in canceling the CM voltage at the motor input, due to the maximization of the filter insertion loss (IL) for the case under study [9], [26]. The main features of the chosen topology are summarized in Table I.

The performance of the topology shown in Fig. 1 is improved by an additional feed-forward action, based on the injection of a signal proportional to the motor CM current, as proposed in this paper. A further improvement is achieved by the reduction of the filter supply voltage and a proper redesign of voltage detection and injection systems, as explained in the following.

Main Features of the Feedback Voltage-Sensing Voltage-Compensating Active Filter

| Amplifier gain | Insertion Loss (IL) | Condition for Maximum IL |
|---|---|---|
| $v_c = -Av_r$ | $1 + \frac{z_r}{z_r + z_s} \cdot A$ | $z_r >> z_s$ |

### B. Improvement of Voltage Detection and Injection Systems

The CM voltage ($V_{\mathrm{CM}}$) to be compensated is detected at the noise receiver (the motor) and compared with the desired $V_{\mathrm{CM}}$ output, set to zero; the error signal is suitably processed by a feedback action, then it is amplified and injected to compensate the $V_{\mathrm{CM}}$. In order to perform an optimal compensation, the proposed circuit should be able to follow the rapid transitions due to the inverter switching. This implies the use of a power amplification stage which is characterized by high slew rate and high gain/bandwidth product (GBW). Actually, it represents the bottleneck of the system. A high GBW is bound to the availability on the market. In general, the smaller is the amplifier supply voltage, the higher is its GBW. Therefore, a reduction of the operating voltage within the filter is advantageous. It can be obtained by a suitable modification of CM voltage detection and injection systems. In particular, to reduce the operating voltage of the filter by a factor $k$, the detected CM voltage has to be divided by $k$ and the injected compensating voltage has to be multiplied by the same factor. Since a voltage-sensing scheme usually adopts a detection system constituted by three wye-connected capacitors $C_d$ [26], a further capacitor $C_1 = 3C_d(k-1)$ is used to detect a suitably divided CM voltage [24]. This calls for a voltage injection system with the capability to multiply the compensating voltage by $k$. Since a CM transformer (CMT) is used for the voltage injection, a CMT with a turn ratio $1{:}k$ is realized. It should be observed that the turn ratio of the CMT is obtained by the minimum turns number at the primary winding, provided that the core saturation is avoided. In this way, small dimensions of the CMT are possible and the desired optimization of the power to size ratio is accomplished.

### C. Feed-Forward Action by CM Current Estimation

Within a feedback compensation system, a slight difference in the slope of the compensating voltage step is observed compared to the actual CM voltage step. This difference is mainly due to the limitation of the amplifier bandwidth but also to the delay of feedback signals propagation. As a consequence, a residual disturbance at the motor terminals, after the introduction of the active filter, is noticed. The residual disturbance exhibits a pulse-shaped waveform similar to the motor CM current. Therefore, by taking a supplementary signal proportional to the motor CM current and adding it directly to the error signal, it is possible to compensate the delay of feedback signals propagation minimizing the residual disturbance. The additional signal can be obtained by a suitable estimation of the motor CM current by sensing the CM voltage at the inverter terminals and applying it to

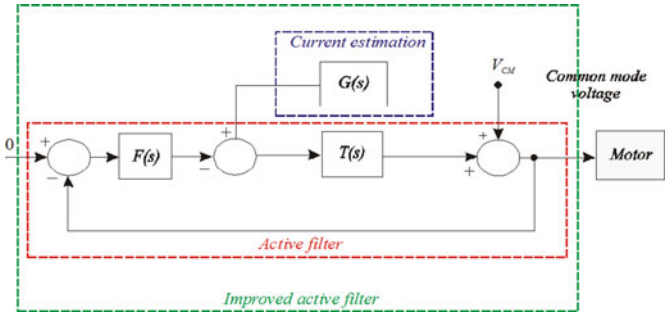


Fig. 2. Schematic configuration of the improved CM active filter.

a simple equivalent circuit reproducing the CM high-frequency motor impedance. In practice, the need for the knowledge of the CM high-frequency motor model is not a limitation, since the most relevant CM phenomenon, to be reproduced, is tied to the front-end capacitance toward ground. Therefore, the motor model can be approximated by only this capacitance, whose value is nearly constant for induction motors belonging to a given rated power class, as demonstrated in [31]. With the proposed approach, the additional signal is built starting from the CM voltage taken directly at the inverter's terminals by a capacitive detector. The performance improvement of the active filter with the addition of the feed-forward action based on the CM current estimation is proven by a frequency-domain analysis (see Section III) where the behavior of the circuit with/without the feed-forward action is compared.

Fig. 2 shows a block diagram of the proposed active filter, where $F(s)$ is a low-pass filter, $T(s)$ is a transfer function, including a linear amplifier, a power amplifier, and a common-mode transformer (CMT) and $G(s)$ is the transfer function of the CM current estimator. Each block is described in detail in the next section.

## III. Frequency-Domain Analysis of the Active Filter

The main components of the active filter are the CMT and the power amplifier. The CMT is used to inject the compensation voltage into the power lines, the power amplifier is necessary to supply the primary winding of the CMT. An auxiliary linear amplifier is used to increase the error signal amplitude maintaining the power amplifier gain close to one. This last condition is necessary to optimally exploit the power amplifier bandwidth.

Finally, a low-pass filter introduces a further real pole that, together with the power amplifier real pole, by a suitable open-loop transfer function gain, can give a couple of complex conjugate poles in the closed loop transfer function.

The transfer functions of the different sections of the active filter are described in Table II.

Usually, the high-frequency pole of the CMT is quite higher than the highest frequency pole of the power amplifier. This occurs since the power amplifier bandwidth is limited to avoid oscillations, whereas the CMT is realized with a suitable magnetic material guaranteeing a high bandwidth. This hypothesis will be experimentally verified, as explained in Section V.

TABLE II
Detail of the Active Filter Sections Transfer Functions

| Filter section | Description | Transfer function |
|---|---|---|
| $F(s)$ | Low pass filter | $F(s)=\frac{p_F}{(s+p_F)}$ |
| $T(s)=T_{LA}(s)T_{PA}(s)T_{CMT}(s)$ | Linear amplifier | $T_{LA}(s)=G_{LA}$ |
| | Power amplifier | $T_{PA}(s)=G_{PA}\frac{p_{PA}}{(s+p_{PA})}$ |
| | CMT | $T_{CMT}(s)=\frac{p_2 s}{(s+p_1)(s+p_2)}$ |
| $G(s)$ | CM current estimator | $G(s)=G_e\frac{s}{s+p_e}$ |

Therefore, under this assumption, it is possible to introduce an approximation according to which

$$T(s) \cong G_{\mathrm{LA}} G_{\mathrm{PA}} \frac{p_{\mathrm{PA}} \cdot s}{(s+p_{\mathrm{PA}})(s+p_1)}. \quad (1)$$

As for the transfer function of the CM current estimator, it should be observed that the pole $p_e$ can be set to a much higher value than the highest harmonic of the CM voltage to be compensated. Then, the following approximation can be assumed for $G(s)$:

$$G(s) \cong G_e s. \quad (2)$$

On such a basis, the transfer function between the CM voltage generated by the PWM inverter and the CM voltage at the input of the motor of the active filter is determined with/without the CM current estimator. In particular, the transfer function of the active filter without the CM current estimator is given in (3), as shown at the bottom of the next page. whereas the transfer function of the active filter with the CM current estimator is given in (4), as shown at the bottom of the next page.

It is possible to note that the introduction of the feed-forward action due to the CM current estimator affects neither the number and values of poles nor the number of zeros of the active filter transfer function. As a matter of fact, the denominator remains unchanged as well as the degree of the numerator. On the other hand, the zeros displacement is influenced by the choice of the CM current estimator parameters. A suitable selection of such parameters makes it possible to perform a stronger attenuation of $V_{\mathrm{CM}}$.

The detailed design of the active filter is described in Section V, together with a numeric comparison between (3) and (4)

## IV. HF Motor Parameters Identification for CM Current Estimation

As anticipated in Section II-C, the CM motor behavior is predominantly capacitive in the whole frequency range under consideration. Anyway, for the sake of completeness, the

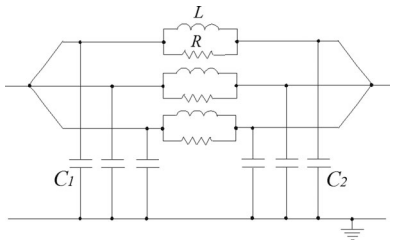


Fig. 3. CM high-frequency circuit model of the motor.

TABLE III
HF PARAMETERS OF THE MOTOR

| Parameter | Value |
|---|---|
| R | 1804 Ω |
| L | 0.144 mH |
| $C_1$=$C_2$=$C$ | 140 pF |

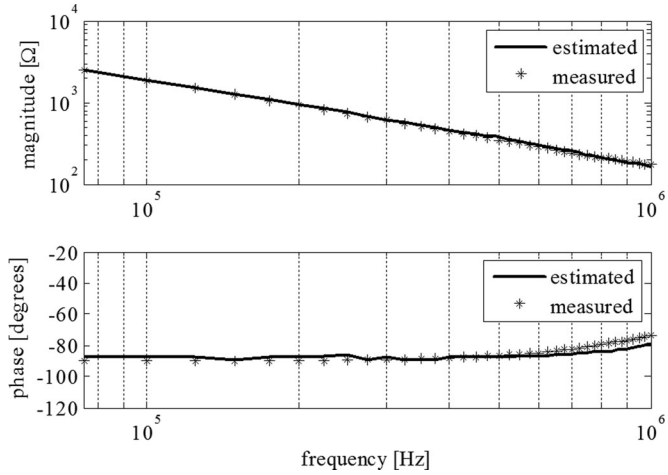


Fig. 4. Estimated and measured motor impedance vs. frequency.

CM high-frequency model of the motor has been identified. In particular, the motor has been modeled using the circuit topology shown in Fig. 3, whose parameters have been identified by using the frequency response of the motor CM impedance. The impedance has been measured between the three phases terminals of the motor connected together and the ground connection, up to 1 MHz, using the Rohde&Schwarz vector network analyzer ZVER. The $R, L, C_1$, and $C_2$ (where $C_1 = C_2 = C$) circuit parameters have been identified using a fitting function embedded in MATLAB [32], [33]. The obtained HF parameters of the motor circuit model are reported in Table III. Fig. 4 shows the matching between estimated and measured frequency responses of the motor impedance.

## V. CM ACTIVE FILTER DESIGN

The electrical scheme of the overall active filter is shown in Fig. 5. It uses a detection system formed of three star-connected capacitors, whose values are $C_d = 1$ nF and a supplementary partition capacitance with a value of 3 nF.

This comes from the choice to divide the detected voltage by a factor $k = 2$ and so to operate the active filter with a voltage that is half the dc supply drive voltage, i.e., about ±18 V.

The linear amplifier is realized by the LM6172 IC having the following features: slew rate 3000 V/$\mu$s and unity-gain bandwidth equal to 100 MHz.

The power amplifier is a LME 49600. It has a rated supply voltage up to ±18 V, a slew rate of 2000 V/$\mu$s and a bandwidth of 180 MHz. It should be noted that more performing amplifiers supplied at lower voltages are not available; then, it is not worth further increasing $k$.

It should be noted that the used amplifiers have a fast enough time response to achieve a good compensation. In particular, the rise time of the CM voltage, experimentally measured, is about 900 ns that corresponds to a maximum frequency of about 350 kHz in the CM voltage spectrum. On this basis, the bandwidth of the power amplifier has been limited to 500 kHz (experimentally verified).

As for the CMT, a single core of nanocrystalline material with very high magnetic permeability (VITROPERM W523) has been used with a turn ratio 1:2 and realized setting 5 turns on the primary winding and 10 turns for each secondary winding; this is aimed at retrieving the dc drive supply voltage level.

The bandwidth of the CMT is about 10 MHz with a low-frequency pole at about 10 kHz [26]; it has been experimentally measured using the test rig described in [25].

As for the low-pass filter, it uses the same amplifier LM6172 in inverting configuration as well as the linear amplifier that implements the sum between the signals coming from the low-pass filter and the CM current estimator.

This estimator is obtained applying the CM voltage to an equivalent circuit reproducing the CM motor impedance. In

$$H(s) = \frac{1}{1+F(s)T(s)} = \frac{(s+p_F)(s+p_1)(s+p_{\mathrm{PA}})}{(s+p_F)(s+p_1)(s+p_{\mathrm{PA}}) + s \cdot p_F G_{\mathrm{PA}} p_{\mathrm{PA}} G_{\mathrm{LA}}}$$
$$= \frac{s^3 + s^2(p_1 + p_{\mathrm{PA}} + p_F) + s[p_1 p_{\mathrm{PA}} + p_F(p_1 + p_{\mathrm{PA}})] + p_1 p_{\mathrm{PA}} p_F}{s^3 + s^2(p_1 + p_{\mathrm{PA}} + p_F) + s[p_1 p_{\mathrm{PA}} + p_F(p_1 + p_{\mathrm{PA}}) + p_F G_{\mathrm{PA}} p_{\mathrm{PA}} G_{\mathrm{LA}}] + p_1 p_{\mathrm{PA}} p_F} \quad (3)$$

$$H_e(s) = \frac{1+G(s)T(s)}{1+F(s)T(s)} = \frac{(s+p_F)(s+p_1)(s+p_{\mathrm{PA}}) + s^2(s+p_F)(G_s G_{\mathrm{PA}} p_{\mathrm{PA}} G_{\mathrm{LA}})}{(s+p_F)(s+p_1)(s+p_{\mathrm{PA}}) + s \cdot p_F G_{\mathrm{PA}} p_{\mathrm{PA}} G_{\mathrm{LA}}}$$
$$= \frac{s^3(1 + G_s G_{\mathrm{PA}} p_{\mathrm{PA}} G_{\mathrm{LA}}) + s^2(p_1 + p_{\mathrm{PA}} + p_F + G_s G_{\mathrm{PA}} p_{\mathrm{PA}} G_{\mathrm{LA}} p_F) + s[p_1 p_{\mathrm{PA}} + p_F(p_1 + p_{\mathrm{PA}})] + p_1 p_{\mathrm{PA}} p_F}{s^3 + s^2(p_1 + p_{\mathrm{PA}} + p_F) + s[p_1 p_{\mathrm{PA}} + p_F(p_1 + p_{\mathrm{PA}}) + p_F G_{\mathrm{PA}} p_{\mathrm{PA}} G_{\mathrm{LA}}] + p_1 p_{\mathrm{PA}} p_F}. \quad (4)$$

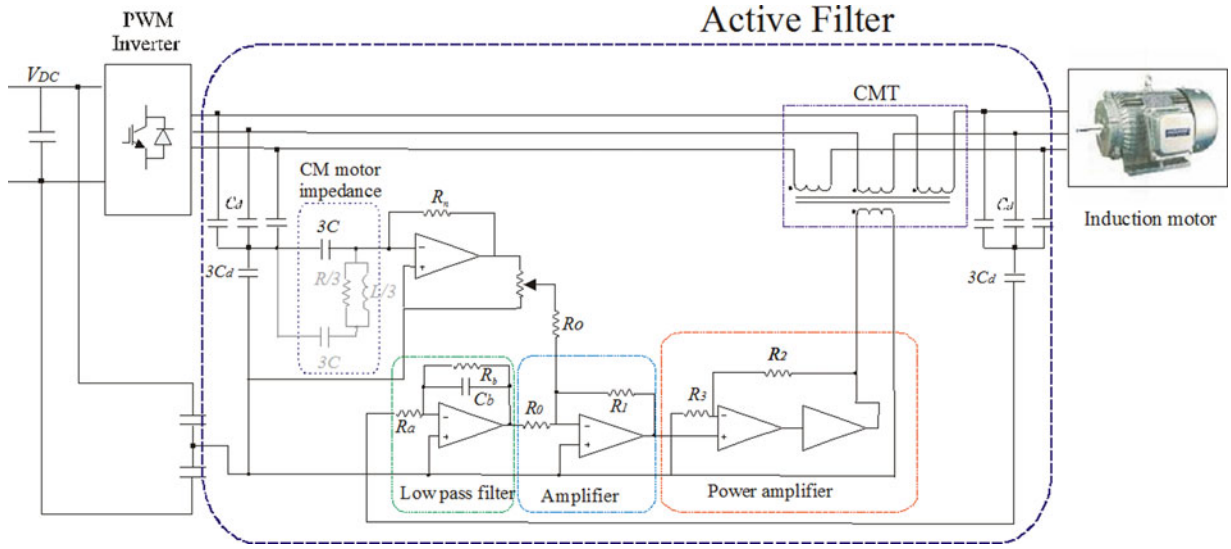


Fig. 5. Circuit scheme of the improved active filter inserted in PWM induction motor drive.

TABLE IV
ACTIVE FILTER SECTIONS PARAMETERS

| Filter section | Gain | Zero(s) | Pole(s) |
|---|---|---|---|
| Low pass filter | $p_F = \frac{1}{R_b C_b}$ | None | $p_F = \frac{1}{R_b C_b}$ |
| Linear amplifier | $G_{LA} = -\frac{R_1}{R_0}$ | None | None |
| Power amplifier | $G_{PA} = -\frac{R_2}{R_3}$ | None | $P_{PA}$ (experimentally determined) |
| CMT | $p_2$ | One zero at the origin | $p_2, p_1$ (experimentally determined) |
| CM current estimator | $G_e$ | One zero at the origin | $p_e = \frac{1}{R_n 3C}$ (neglected) |

TABLE V
ACTIVE FILTER ELECTRICAL COMPONENT VALUES

| Section | Parameter | Value |
|---|---|---|
| Low pass filter | $R_b$ | 10 kΩ |
| | $C_b$ | 180 pF |
| | $R_a$ | 10 kΩ |
| Linear amplifier | $R_1$ | 10 kΩ |
| | $R_0$ | 10 kΩ |
| Power amplifier | $R_3$ | 10 kΩ |
| | $R_2$ | 20 kΩ |
| CM current estimator | $3C$ | 420 pF |
| | $R_n$ | 1 kΩ |

particular, the input capacitance 3 $C$ and the feedback resistance $R_n$ give a transfer function with a zero in the origin and a high-frequency pole (at $f = 1/3R_n$C) realizing the behavior of a real differentiator. Finally, the variable resistance gives an additional gain corresponding to the $G_s$ parameter indicated in Table IV. The chosen power amplifier and core magnetic material allow a very compact filter layout.

The used circuit parameters are reported in Table V.

Table IV gives, for each filter section, the expression of the corresponding parameters.

On the basis of the parameters of the active filter, the transfer functions in (3) and (4) are calculated to compare the circuit behavior without and with the contribution of the feed-forward action due to the CM current estimator. This comparison is shown in Fig. 6 where the Bode plots of transfer functions (3) and (4) are given. It is possible to observe that the introduction of the feed-forward action leads to a stronger attenuation of the CM voltage in the range of frequency between about $125 \times 10^3$ rad/s and about $4.5 \times 10^6$ rad/s. As for the pole–zero displacement of functions $H(s)$ and $H_e(s)$, it should be observed that both functions exhibit the same denominator; then, pole distribution is not affected by the introduction of the current estimator. On the other hand, the zero distribution is modified with the aim to emphasize the pole attenuating action at the frequencies of interest. In particular, the introduction of the current estimator implies the increase of a zero value, as shown in Fig. 7 and Table VI.

## VI. EXPERIMENTAL ARRANGEMENT

The proposed CM EMI active filter is intended for a vehicular motor drive. The system under test is composed of a demo board with an Altera EP3C25F324C8 FPGA, suitably programmed in VHDL to implement the control of a 42 V 1.1 kW induction motor by means of an integrated IGBT inverter (STGIPS10K60 A), with a switching frequency of 20 kHz. The experimental arrangement of the active filter is realized according to the design criteria given in the previous section.

The power amplifier can reproduce the CM voltage to be applied to the primary of CMT with the required current, as shown in Fig. 8. Moreover, the vertical scales of the two waveforms

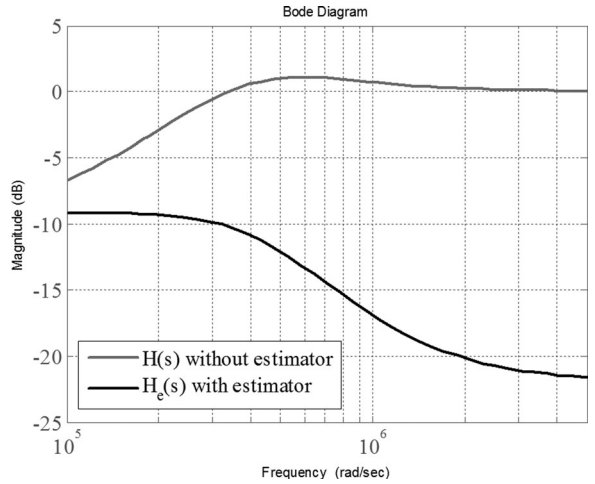


Fig. 6. Comparison between the attenuation obtained without the estimator (grey line) and with the estimator (black line).

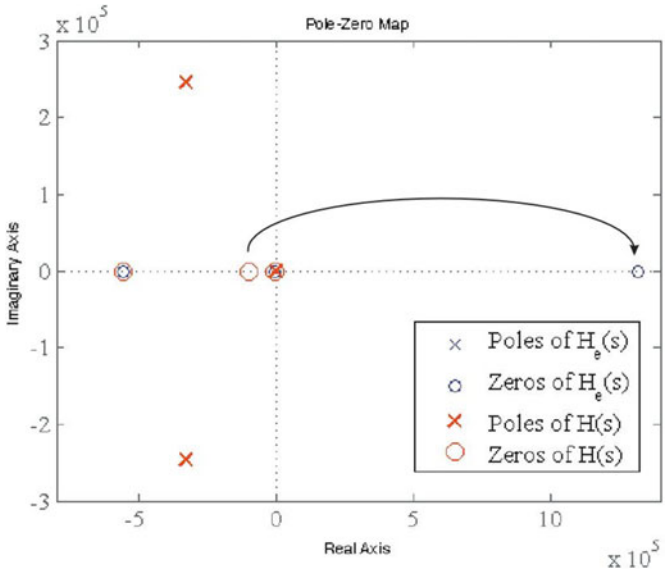


Fig. 7. Pole–zero displacement without the estimator and with the estimator.

TABLE VI
POLE–ZERO VALUES OF $H(s)$ AND $H_e(s)$

| Poles x10$^5$ rad/sec | Zeros w/o estimator x10$^5$ rad/sec | Zeros with estimator x10$^5$ rad/sec |
|---|---|---|
| -3.2946+i2.4560 | -1.0000 | 13.1720 |
| -3.2946-i2.4560 | -5.5556 | -5.5556 |
| -0.0165 | -0.0500 | -0.0470 |

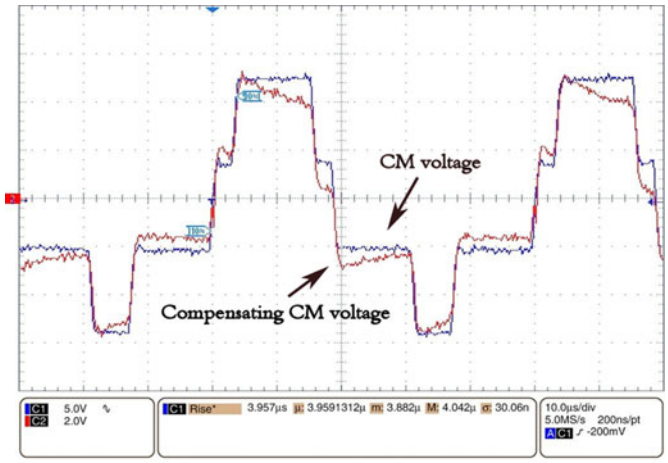


Fig. 8. Comparison between the CM voltage and the compensating CM voltage at the primary of the CMT. Time division: 10 $\mu$s/div. CM voltage: 5 V/div. Compensating CM voltage: 2 V/div.

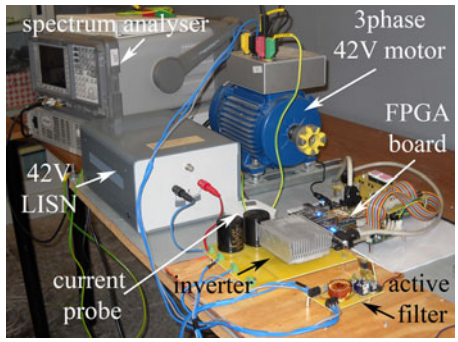


Fig. 9. Experimental rig.

Fig. 10. Active filter.

are different; the voltage applied to the primary of the CMT is increased by the turn ratio of the same CMT before being subtracted from the $V_{\mathrm{CM}}$ generated by the inverter. In Figs. 9 and 10, photos of the experimental arrangement and of the active filter prototype are shown, respectively. It is worth noting that to set up the proposed circuit a power OA with a high bandwidth and high slew rate is needed. There are some suitable components on the market however it is often necessary to lessen the rated bandwidth to avoid oscillations as suggested by the OA manufacturers. The layout of the PCB should be obtained as a tradeoff between compactness and the need for avoiding parasitic coupling among wires of the circuit. The use of SMD components makes the circuit more compact but requires a particular care for the layout design. Finally the gain of the CM current estimator is a critical parameter: it should be as high as possible without causing oscillations. In the prototype realization

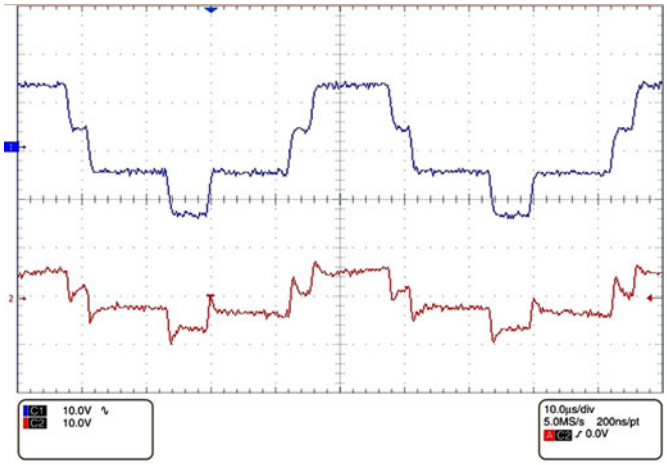


Fig. 11. CM voltage without the active filter (upper line) and with the active filter without feed-forward signal by CM current estimation (lower line). Time division: 10 $\mu$s/div. Vertical axis: 10 V/div.

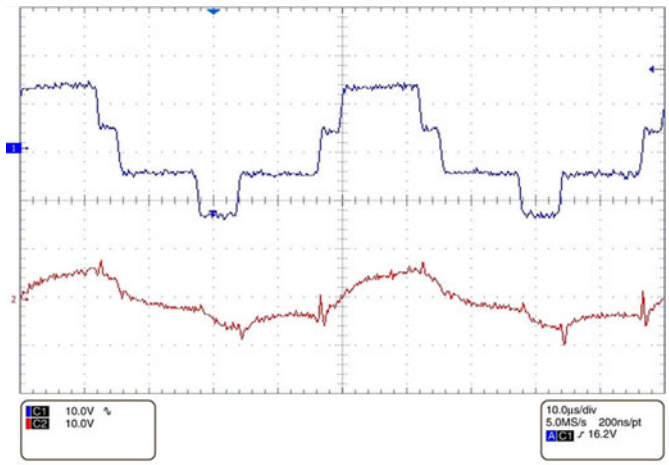


Fig. 12. CM voltage without the active filter (upper line) and with the active filter with feed-forward signal by CM current estimation (lower line). Time division: 10 $\mu$s/div. Vertical axis: 10 V/div.

it has been obtained by a variable resistance set manually to compensate possible tolerance of other circuit components.

## VII. Experimental Results

A digital oscilloscope (Tektronix TDS7254B) has been used to capture the time domain waveforms. As for the time domain current measurements, the exploited system includes an amplifier (Tektronix TCPA 300) and a current probe with a bandwidth of 50 MHz (Tektronix A6303). The frequency-domain measurements have been performed using a spectrum analyzer (Agilent E4402B), a current probe (Rohde&Schwarz EZ-17), and a voltage transducer. These measurements cover the range between 10 kHz and 1 MHz.

Fig. 11 shows the time waveforms of the CM voltages at the motor terminals without any filter and with the proposed filter when no feed-forward signal is added. It is possible to observe that the CM voltage amplitude with the filter is reduced to about 50%. In principle, a better compensation could be obtained by increasing the gain of the linear amplifier $G_{\mathrm{LA}}$. However, this choice leads to higher imaginary values of the complex conjugate poles, decreasing the damping. In addition, with a higher value of $G_{\mathrm{LA}}$, the high-frequency attenuation is worsened. Therefore, the proposed results come from the best tradeoff between low- and high-frequency performance of the active filter.

The power amplifier can reproduce the CM voltage to be applied to the primary of CMT with the required current, as shown in Fig. 8.

When the feed-forward current signal is introduced, a smoothing of the CM voltage edges is further observed, as shown in Fig. 12. As a matter of fact, the feed-forward signal, corresponding to the estimated current, correctly reproduces the rapid edges of the motor CM current, thus contributing to an improved compensation of the CM voltage. This is illustrated in Fig. 13, where the comparison between the estimated current and the CM motor current is shown.

Fig. 14 shows the frequency spectrum of the motor CM voltage without the active filter. A series of peaks corresponding to

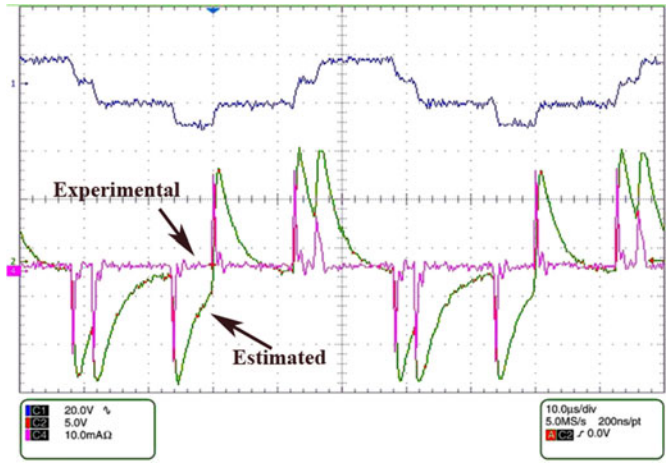


Fig. 13. CM voltage without the active filter (upper line) and comparison between the motor CM current and the estimated CM current. Time division: 10 $\mu$s/div. Vertical axes: upper line 20 V/div; Experimental CM current 5 V/div; Estimated CM current: 10 mA/div.

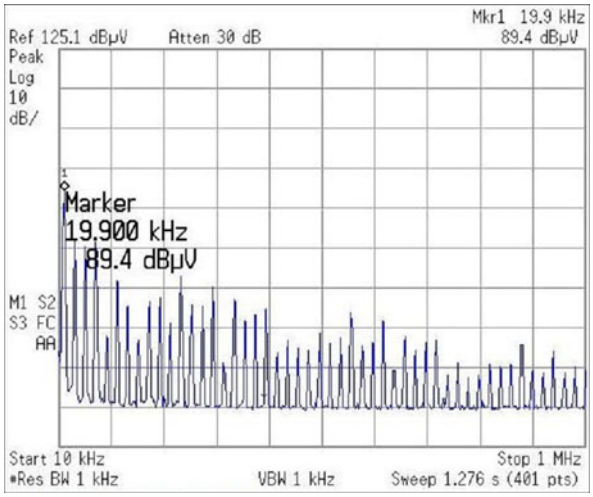


Fig. 14. Spectrum of the CM voltage without the active filter.


Fig. 15. Spectrum of the CM voltage with the active filter without feed-forward signal by CM current estimation.

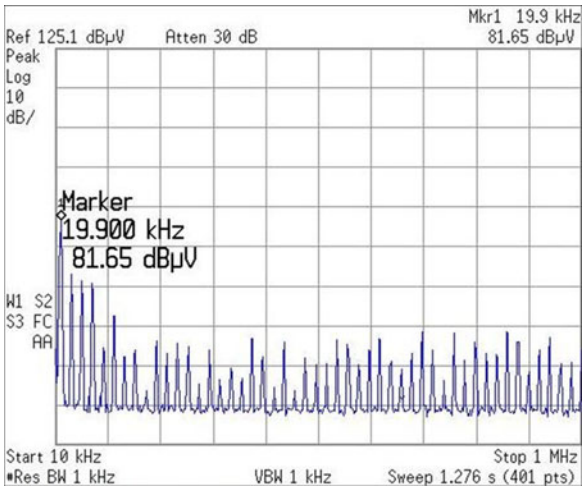


Fig. 16. Spectrum of the CM voltage with the active filter with feed-forward signal based on CM current estimation.

the inverter switching frequency and its harmonics is clearly observable. The peak at 20 kHz has an amplitude equal to 89.4 dB·$\mu$V that corresponds to about 9.3 V, due to the presence of an input attenuator giving an attenuation of about 50 dB.

Figs. 15 and 16show the frequency spectra of the motor CM voltage with the active filter when no feed-forward current signal injection is present and when this injection is performed, respectively. From Fig. 15, it is clear that the feedback filter action produces a reduction of the low frequency peaks. In particular, the 20 kHz peak exhibits a reduction of 8 dB. Consequently, the new amplitude of the CM voltage is about 3.8 V. The effect of the introduction of the additional signal, shown in Fig. 16, is a reduction of frequency components higher than 100 kHz of the CM voltage spectrum, as expected. A comparison of the motor CM currents spectra without any active filter and with the proposed circuit, without and with the feed-forward current action, is possible by observing Figs. 17–19. In particular, it is clear that, when no feed-forward current action is applied, the introduction of the active filter leads to a slight reduction of the CM current frequency spectrum; this is coherent with the

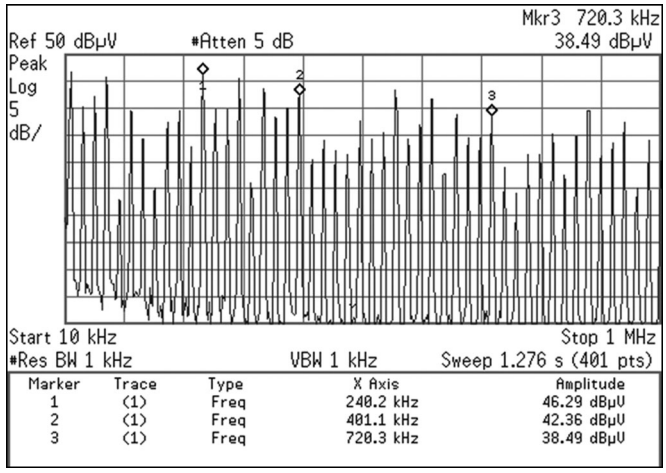


Fig. 17. Spectrum of the CM current without the active filter.

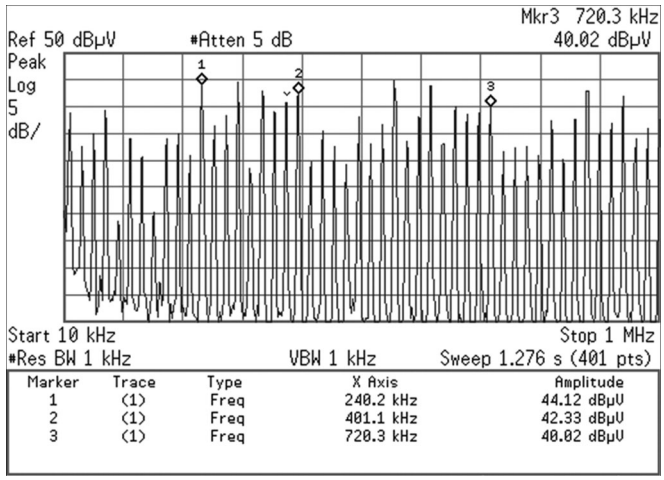


Fig. 18. Spectrum of the motor CM current with the active filter without feed-forward signal by CM current estimation.

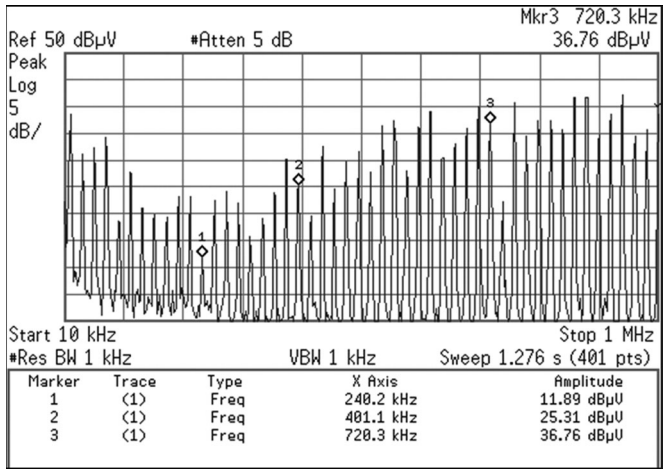


Fig. 19. Spectrum of the motor CM current with the active filter with feed-forward signal based on CM current estimation.

TABLE VII
SQUARE SUM OF THE CM CURRENT HARMONIC AMPLITUDES RATIO

| Active Filter configuration | $\alpha$ |
|---|---|
| Without feed-forward action | 0.87 |
| With feed-forward action | 0.35 |

primary scope of an output CM filter, i.e., the reduction of the motor bearing stress.

On the contrary, when the feed-forward current action is added, a significant reduction of the CM current frequency content ranging between 20 and 750 kHz is achieved, thus improving the filter performance also in terms of EMI reduction. This result is consistent with the theoretical analysis of the active filter with and without the CM current estimator expressed by the comparison shown in Fig. 6. In order to give a quantitative evaluation of such an EMI reduction, a comparison of the square sum of the CM current harmonic amplitudes in the two considered filter configurations referred to the CM current without any filter is given in Table VII. In particular, the following quantity has been evaluated in the two filter configurations:

$$\alpha = \frac{\sum_n I^2_{n\_\mathrm{cm}f}}{\sum_n I^2_{n\_\mathrm{cm}}} \tag{5}$$

where $I_{n\_\mathrm{cm}}$ is the $n$th harmonic component of the CM current without any filter and $I_{n\_\mathrm{cm}f}$ is the $n$th harmonic component of the CM current the active filter without or with feed-forward action. It should be observed that, for a given layout, $\alpha$ in (5) gives a measure of the reduction of the energy content associated to CM EMI. From Table VII, it is possible to observe that the introduction of the active filter scheme without the additional feed-forward current action leads to a reduction of the EMI of about 13%, whereas the introduction of the active filter scheme with the additional feed-forward current action leads to a reduction of about 65%.

## VIII. CONCLUSION

The paper presents a novel CM active filter for vehicle dc-fed motor drives. The filter scheme is based on a voltage feedback action with an optimized design of the CM voltage detection/injection systems. Moreover, it uses an additional feed-forward signal obtained by a suitable estimation of the motor CM current which improves the performance in terms of EMI reduction. The effectiveness of the improved active filter is theoretically demonstrated. The filter is experimentally set up using linear amplifiers that allow an efficient and compact realization. The experimental investigation shows a reduction of the CM EMI in the frequency range of interest.

## REFERENCES

[1] R. Jayabalan, B. Fahimi, A. Koenig, and S. Pekarek, "Applications of power electronics-based systems in vehicular technology: State of the art and future trends," presented at 35th Annu. Power Electron. Spec. Conf., Aachen, Germany, 2004.
[2] J. G. Kassakian, H.-C. Wolf, and C. J. Hurton, "Automotive electrical systems circa 2005," *IEEE Spectr.*, vol. 33, no. 8, pp. 22–27, Aug. 1996.
[3] S. C. Smithson and S. S. Williamson, "Constant power loads in more electric vehicles—An overview," in *Proc. 38th Annu. Conf. IEEE Ind. Electron. Soc.*, 2012, pp. 2914–2922.
[4] A. Emadi, Y. J. Lee, and K. Rajashekara, "Power electronics and motor drives in electric, hybrid electric, and plug-in hybrid electric vehicles," *IEEE Trans. Ind. Electron.*, vol. 55, no. 6, pp. 2237–2245, Jun. 2008.
[5] M. M. Jalla, A. Emadi, G. A. Williamson, and B. Fahimi, "Modeling of multiconverter more electric ship power systems using the generalized state space averaging method," in *Proc. 30th Annu. Conf. IEEE Ind. Electron. Soc.,*, 2004, vol. 1, pp. 508–513.
[6] S. Chen, T. A. Lipo, and D. Fitzgerald, "Source of induction motor bearing currents caused by PWM inverters," *IEEE Trans. Energy Conv.*, vol. 11, no. 1, pp. 25–32, Mar. 1996.
[7] A. Muetze and A. Binder, "Calculation of circulating bearing currents in machines of inverter-based drive systems," *IEEE Trans. Ind. Electron.*, vol. 54, no. 2, pp. 932–938, Apr. 2007.
[8] A. Muetze and A. Binder, "Pratical rules for assessment of inverter-induced bearing currents in inverter-fed AC motors up to 500 kW," *IEEE Trans. Ind. Electron.*, vol. 54, no. 3, pp. 1614–1622, Jun. 2007.
[9] Y.-C. Son and S.-K. Sul, "Generalization of active filters for EMI reduction and harmonic compensation," *IEEE Trans. Ind. Appl.*, vol. 42, no. 2, pp. 545–551, Mar./Apr. 2006.
[10] K. Mainali and R. Oruganti, "Conducted EMI mitigation techniques for switch-mode power converters: A survey," *IEEE Trans. Power Electron.*, vol. 25, no. 9, pp. 2344–2356, Sep. 2010.
[11] W. Chen, W. Zhang, X. Yang, Z. Sheng, and Z. Wang, "An experimental study of common and differential mode active EMI filter compensation characteristics," *IEEE Trans. Electrom. Compat.*, vol. 51, no. 3, pp. 683–691, Aug. 2009.
[12] N. Mutoh, M. Nakanishi, M. Kanesaki, and J. Nakashima, "EMI noise control methods suitable for electrical vehicles drive systems," *IEEE Trans. Electromagn. Compat.*, vol. 47, no. 4, pp. 930–937, Nov. 2005.
[13] V. Serrao, A. Lidozzi, and A. Di Napoli, "EMI filters architectures for power electronics in hybrid vehicles," in *Proc. Power Electron. Spec. Conf.*, Jun. 15–19, 2008, pp. 3098–3103.
[14] N. Mutoh and M. Kanesaki, "A suitable method for ecovehicles to control surge voltage at motor terminals connected to PWM inverters and to control induced EMI noise," *IEEE Trans. Veh. Technol.*, vol. 57, no. 4, pp. 2089–2098, Jul. 2008.
[15] Y. Maillet, L. Rixin, S. Wang, F. Wang, R. Burgos, and D. Boroyevich, "High-density EMI filter design for DC-fed motor drives," *IEEE Trans. Power Electron.*, vol. 25, no. 5, pp. 1163–1172, May 2010.
[16] H.-F. Chen, C.-Y. Yeh, and K.-H. Lin, "A method of using two equivalent negative inductances to reduce parasitic inductances of a three-capacitor EMI filter," *IEEE Trans. Power Electron.*, vol. 24, no. 12, pp. 2867–2872, Dec. 2009.
[17] J. Biela, A. Wirthmueller, R. Waespe, M. L. Heldwein, K. Raggl, and J. W. Kolar, "Passive and active hybrid integrated EMI filters," *IEEE Trans. Power Electron*, vol. 24, no. 5, pp. 1340–1349, May 2009.
[18] S. Wang, Y. Y. Maillet, F. Wang, D. Boroyevich, and R. Burgos, "Investigation of hybrid EMI filters for common-mode EMI uppression in a motor drive system," *IEEE Trans. Power Electron.*, vol. 25, no. 4, pp. 1034–1045, Apr. 2010.
[19] Y.-C. Son and S.-K. Sul, "A new active common-mode EMI filter for PWM inverter," *IEEE Trans. Power Electron.*, vol. 18, no. 6, pp. 1309–1314, Nov. 2003.
[20] S. Ogasawara, H. Ayano, and H. Akagi, "An active circuit for cancellation of common-mode voltage generated by a PWM inverter," *IEEE Trans. Power Electron*, vol. 13, no. 5, pp. 835–841, Sep. 1998.
[21] S. Ogasawara, H. Ayano, and H. Akagi, "An active circuit for cancellation of common-mode voltage generated by a PWM inverter," *IEEE Trans. Power Electron.*, vol. 13, no. 5, pp. 835–841, Sep. 1998.
[22] S. Ogasawara and H. Akagi, "Circuit configurations and performance of the active common-noise canceller for reduction of common-mode voltage generated by voltage-source PWM inverters," in *Proc. IEEE Ind. Appl. Conf.*, Oct. 8–12, 2000, vol. 3, pp. 1482–1488.
[23] C. Mei, J. C. Balda, and W. P. Waite, "Cancellation of common-mode voltages for induction motor drives using active method," *IEEE Trans. Energy Conv.*, vol. 21, no. 2, pp. 380–386, Jun. 2006.
[24] M. C. Di Piazza, G. Tinè, and G. Vitale, "An improved active common mode voltage compensation device for induction motor drives," *IEEE Trans. Ind. Electron.*, vol. 55, no. 4, pp. 1823–1834, Apr. 2008.

[25] M. C. Di Piazza, A. Ragusa, and G. Vitale, "Effects of common mode active filtering in induction motor drives for electric vehicles," *IEEE Trans. Veh. Thecnol.*, vol. 59, no. 6, pp. 2664–2673, Jul. 2010.
[26] M. C. Di Piazza, A. Ragusa, and G. Vitale, "An optimized feedback common mode active filter for vehicular induction motor drives," *IEEE Trans. Power Electron.*, vol. 26, no. 11, pp. 3153–3162, 2011.
[27] M. C. Di Piazza, M. Luna, A. Ragusa, and G. Vitale, "An improved common mode active filter for EMI reduction in vehicular motor drives," presented at IEEE Vehicle Power Propulsion Conf., Chicago, IL, USA, Sep. 2011.
[28] M. C. Di Piazza, A. Ragusa, and G. Vitale, "Design of grid-side electromagnetic interference filters in AC motor drives with motor-side common mode active compensation," *IEEE Trans. Electromagn. Compat.*, vol. 51, no. 3, pp. 673–682, Aug. 2009.
[29] A. von Jouanne, D. A. Rendusara, P. N. Enjeti, and J. W. Gray, "Filtering techniques to minimize the effect of long motor leads on PWM inverter-fed AC motor drive systems," *IEEE Trans. Ind. Appl.*, vol. 32, no. 4, pp. 919–926, Jul./Aug. 1996.
[30] L. Lawhite and M. F. Schlecht, "Design of active ripple filters for power circuits operating in the 1–10 MHz range," *IEEE Trans. Power Electron.*, vol. 3, no. 3, pp. 310–317, Jul. 1988.
[31] A. Boglietti, A. Cavagnino, and M. Lazzari, "Experimental high-frequency parameter identification of AC electrical motors," *IEEE Trans. Ind. Appl.*, vol. 43, no. 1, pp. 23–29, Jan./Feb. 2007.
[32] E. C. Levi, "Complex-curve fitting," *IRE Trans. Automat. Control*, vol. AC-4, no. 1, pp. 37–44, May 1959.
[33] A. Carrubba, M. C. Di Piazza, G. Tinè, and G. Vitale, "Evaluation of common mode disturbance mitigation devices in AC motor drives through HF modelling," presented at IEEE Int. Symp. Ind. Electron., Montreal, QC, Canada, Jul. 9–13 2006.

A. Bhaktha vachala received the B.Tech. degree from PBR VITS in the year 2003 and M.Tech . degree from the JNTU , Hyderabad , India . Also Perusing Ph.D. degree from Jawaharlal Nehru Technological University, Hyderabad. He is working in the area of Electric vehicle applications in transportation systems from last four years. He has been with the Department of Electrical and Electronics Engineering, PBR visvodaya Institute of technology and science, kavali affiliated by JNTU Anatapur since last 10 years , where he is currently an Associate Professor . His research interests include several areas of power electronics and electric vehicle applications of power electronics . He has authored or coauthored several papers in power electronics . He completed a UGC sponsored project worth of 4,60,00/- on electric drives . He is a life member of Indian Society for Technical Education.

E-mail: bhaktha1000@gmail.com

Ms.Nimmakayala Kavitha was born in India .She isPursuing M.Tech Degree in Power electronic inEEE Department in Visvodaya Engineering College,Kavali, SPSR Nellore Dt .Andhra Pradesh State, India .
E-mail: Kavithareddy233@gmail.com.